

Infrared optical response of strongly correlated cuprates: the effects of topological phase separation.

A.S. Moskvina and E.V. Zenkov*
Ural State University, 620083 Ekaterinburg, Russia

Cuprates are believed to be unconventional systems which are unstable with regard to a self-trapping of the low-energy charge transfer excitons with a nucleation of electron-hole (EH) droplets being actually the system of coupled electron CuO_4^{7-} and hole CuO_4^{5-} centers having been glued in lattice due to a strong electron-lattice polarization effects. The hole/electron doping into parent cuprate is likely to be a driving force for a growth of primary EH droplets with a gradual stabilization of a single, or multi-center skyrmion-like EH Bose liquid collective mode, followed by a first order phase transition from parent insulating state into unconventional topological EH Bose liquid phase (EHBL). Nanoscopic electron inhomogeneity is believed to be inherent property of doped cuprates throughout the phase diagram beginning from EH droplets in insulating parent system and ending by a topological phase separation in EHBL phase.

We examine the effects of electron inhomogeneity accompanying such a phase separation on IR optical conductivity. A simple model of metal-insulator composite and effective medium theory has been used to describe the static phase separation effects. The low-frequency dynamics of topological EHBL phase in a random potential in underdoped regime has been discussed in a quasiparticle approximation in frames of the memory function formalism.

The effects of static and dynamic nanoscopic phase separation are believed to describe the main peculiarities of the optical response of doped cuprates in a wide spectral range.

Keywords: cuprates, phase separation, optical conductivity, memory function

I. INTRODUCTION

The nature of the optical response of strongly correlated cuprates is presently still a matter of great controversy. The unconventional behavior of cuprates strongly differs from that of ordinary metals and merely resembles that of a doped semiconductor. Moreover, the history of high T_c 's itself shows that we deal with a transformation of particularly insulating state in which the electron correlations govern the essential physics. New principles must be developed to treat these systems with its non-Fermi-liquid behavior. First of all we have to change the current paradigm of the metal-to-insulator (MI) transition to that of an insulator-to-metal (IM) phase transition. These two approaches imply essentially different starting points: the former starts from a rather simple metal scenario with inclusion of correlation effects, while the latter does from strongly correlated atomic-like scenario with the inclusion of a charge transfer.

The copper oxides start out life as insulators in contrast with BCS superconductors being conventional metals. It is impossible to understand the behavior of the doped cuprates and, in particular, the origin of HTSC unless the nature of the doped insulating state is incorporated into the theory. In particular, the Fermi liquid theory of the normal state and the BCS theory of the superconducting state, which are so successful for conventional metals, were not designed for doped insulators, and they do not apply to the HTSC. Consequently it is necessary to develop a new mechanism and many-body theory of HTSC.

The problem of a doped insulator is sure much more complicated than it is implied in oversimplified ap-

proaches such as an effective t - J -model. First, we deal with effects of electron inhomogeneity and phase separation. These are currently considered to be inherent property of lightly doped or so-called under-doped cuprates. However, recent scanning electron micrography measurements clearly evidence the inherent electron inhomogeneity in optimally doped $\text{Bi}_2\text{Sr}_2\text{CaCu}_2\text{O}_8$.^{1,2}

The emergence of electron inhomogeneity leads to a strong complication of the optical response and its analysis due to a number of specific effects typical for optically inhomogeneous systems. The discussion and modelling of such effects would be the main goal of the paper. Its structure is organized as follows. In Sec.II we discuss the origin and evolution of electron inhomogeneity in doped cuprates. In Sec.III the effective medium theory is applied to describe the optical response of "quenched" electronic inhomogeneity. The effects of the dynamics of multi-center topological defect in a random potential are addressed in Sec.IV.

II. CONDENSATION OF CT EXCITONS AND PHASE SEPARATION IN DOPED CUPRATES

In case of cuprates we deal with systems which conventional ground state seems to be unstable with regard the transformation into a new phase state with a variety of unusual properties. It is worth noting the text-book example of BaBiO_3 system where we unexpectedly deal with the disproportionated $\text{Ba}^{3+} + \text{Ba}^{5+}$ ground state instead of the conventional lattice of Ba^{4+} cations. The bismuthate situation can be viewed as a result of condensation of charge transfer (CT) excitons, in other words, the spontaneous generation of self-trapped CT excitons

in the ground state with a proper transformation of lattice parameters. These problems are closely related with the hidden multistability intrinsic to each solid.³ If the ground state of a solid is pseudo-degenerate, being composed of true and false ground states with each structural and electronic orders different from others, one might call it multi-stable.

In our view, the physics of the doped cuprates, including superconductivity, is driven by a self-trapping of the CT excitons.^{4,5} Such excitons are the result of self-consistent charge transfer and lattice distortion with appearance of the “negative- U ” effect. In contrast with BaBiO₃ system where we deal with a spontaneous generation of self-trapped CT excitons (STE) in the ground state, the parent insulating cuprates are believed to be near excitonic instability when the self-trapped CT excitons form the candidate relaxed excited states to struggle with the conventional ground state.³ In other words, the lattice relaxed CT excited state should be treated on an equal footing with the ground state. If the interaction between STE were attractive and so large that the cohesive energy W_1 per one STE exceeds the energy E_R of one STE, the STE’s and/or its clusters will be spontaneously generated everywhere without any optical excitation, and be condensed to form a new electronic state on a new lattice structure.³

A. Electron-hole droplets in cuprates: pseudo-impurity and phase separation regimes

Cuprates are believed to be unconventional systems which are unstable with regard to a self-trapping of the low-energy charge transfer excitons^{6,7,8} with a nucleation of EH droplets being actually the system of coupled electron CuO_4^{7-} and hole CuO_4^{5-} centers having been glued in lattice due to a strong electron-lattice polarization effects. Phase transition to novel hypothetically metallic state could be realized due to a mechanism familiar to semiconductors with filled bands such as Ge and Si where given certain conditions one observes a formation of metallic EH-liquid as a result of the exciton decay.⁹ However, the system of strongly correlated electron CuO_4^{7-} and hole CuO_4^{5-} centers appears to be equivalent to an electron-hole Bose-liquid (EHBL) in contrast with the electron-hole Fermi-liquid in conventional semiconductors. A simple model description of such a liquid implies a system of local singlet bosons with a charge of $q = 2e$ moving in a lattice formed by hole centers.¹⁰ Local boson in our scenario represents the electron counterpart of Zhang-Rice singlet, or two-electron configuration $b_{1g}^2 A_{1g}$. Naturally, that conventional electron CuO_4^{7-} center represents a relaxed state of a composite system: “hole CuO_4^{5-} center plus local singlet boson”, while the “non-retarded” scenario of a novel phase is assumed to incorporate the unconventional states of electron CuO_4^{7-} center up to its orbital degeneracy.

Homogeneous nucleation implies the spontaneous formation of EH droplets due to the thermodynamic fluctuations in exciton gas. Generally speaking, such a state with a nonzero volume fraction of EH droplets and the spontaneous breaking of translational symmetry can be stable in nominally pure insulating crystal. However, the level of intrinsic non-stoichiometry in oxides is significant (one charged defect every 100-1000 molecular units is common). The charged defect produces random electric field, which can be very large (up to 10^8 Vcm^{-1}) thus promoting the condensation of CT excitons and the nucleation of EH droplets. Deviation from the neutrality of the CuO_2 layers implies the existence of additional electron, or hole centers that can be the natural centers for the *inhomogeneous nucleation* of the EH droplets. Such droplets are believed to provide the more effective screening of the electrostatic repulsion for additional electron/hole centers, than the parent insulating phase. As a result, the electron/hole injection to the insulating cuprate due to a nonisovalent substitution as in $\text{La}_{2-x}\text{Sr}_x\text{CuO}_4$, $\text{Nd}_{2-x}\text{Ce}_x\text{CuO}_4$, or change in oxygen stoichiometry as in $\text{YBa}_2\text{Cu}_3\text{O}_{6+x}$, $\text{La}_2\text{CuO}_{4-\delta}$, $\text{La}_2\text{Cu}_{1-x}\text{Li}_x\text{O}_4$, or field-effect is believed to shift the phase equilibrium from the insulating state to the unconventional electron-hole Bose liquid, or in other words induce the insulator-to-EHBL phase transition.

The optimal way to the nucleation of EH droplets in parent system like La_2CuO_4 , $\text{YBa}_2\text{Cu}_3\text{O}_6$ is to create charge inhomogeneity by nonisovalent chemical substitution in CuO_2 planes or in “out-of-plane stuff”, including interstitial atoms and vacancies. This process results in an increase of the energy of the parent phase and creates proper conditions for its competing with others phases capable to provide an effective screening of the charge inhomogeneity potential. The strongly degenerate system of electron and hole centers in EH droplet is one of the most preferable ones for this purpose. At the beginning (nucleation regime) an EH droplet nucleates as a nanoscopic cluster composed of several number of neighboring electron and hole centers pinned in the CuO_2 plane by disorder potential. Of course, the conditions for such a nucleation are delicately determined by the crystal and chemical surroundings of the CuO_2 planes (“out-of-plane stuff”). Both the electron and hole centers at the atomic-molecular level and the EH droplets at the nanoscopic scale level are the elementary building blocks for an unconventional electron-crystalline structure of the cuprates with the nonisovalent substitution. EH droplet is a nanoscopic center for a pinning of the various quasi-local hybrid charge-spin-vibronic modes with a definite relaxation time and spatially non-uniform DOS distribution or even internal micro-phase separation.

An occurrence of the EH droplets as the domains of the novel phase manifests itself in various properties of the cuprates with a non-isovalent substitution even at the low content of the nucleation centers. On the one hand, main features of this pseudo-impurity regime are determined by the intrinsic properties of the EH

droplets with expected delocalization and metallic-like behavior at $T > T_{CO}$, localization with charge ordering at $T < T_{CO}$, and other phase transformations up to a quasi-local Bose-condensation at $T < T_{BS}$ with an appearance of the superconducting order parameter.¹¹ On the other hand, the real properties of the system will be determined by the peculiar geometrical factors as a relative volume fraction of the EH droplets, their average size and appropriate dispersion, and, possibly, by their form and/or texture. Numerous examples of the unconventional behavior of the cuprates in the pseudo-impurity regime could be easily explained with taking into account the inter-phase boundary effects (coercitivity, the mobility threshold, oscillations, relaxation etc.) and corresponding characteristic quantities. In this connection one should emphasize an occurrence of the characteristic temperatures T_b for the start of the boundaries motion, or for the loss of the stability of either geometrical droplet configuration. In general, such phenomena should accompany any partial phase transition for a phase-separated system, that could result in an appearance of a peculiar doublet structure of the temperature anomalies.

EH droplets can manifest itself remarkably in various properties of the cuprates even at small volume fraction, or in a “pseudo-impurity regime”. Main features of this “pseudo-impurity regime” are determined both by the intrinsic properties of the EH droplets and by the peculiar geometrical factors as a relative volume fraction of droplets, their average size and appropriate dispersion, and, possibly, by their form and/or texture. Numerous examples of the unconventional behavior of the cuprates in the pseudo-impurity regime could be easily explained with taking into account the inter-phase boundary effects (coercitivity, the mobility threshold, oscillations, relaxation etc.) and corresponding characteristic quantities.

Under increasing doping the “pseudo-impurity regime” with a relatively small volume fraction of EH droplets can gradually transform into a micro- (electronic) or macro- (chemical) “phase-separation regime” with a sizeable volume fraction of EH droplets.

The above viewpoint on the phase separation (PS) phenomena in cuprates is, in general, compatible with the pioneer ideas by Emery and Kivelson^{12,13,14} and some other model approaches. So on the basis of the neutron scattering data Egami¹⁵ conjectured an appearance of a nano-scale heterogeneous structure which is composed of a plenty mobile-carrier existing region of metallic conductivity and semi-localized scarce carrier region with antiferromagnetic spin ordering.

Phase separation is now widely discussed as an important phenomenon accompanying the high- T_c superconductivity. The pseudo-impurity regime can be termed as a nanoscopic phase separation. Macroscopic, or chemical phase separation with the x -rays and neutrons detectable domains of a new phase exactly takes place in superoxygenated $\text{La}_2\text{CuO}_{4+\delta}$ ¹⁶, due to the enhanced mobility of negatively charged oxygens which can compensate charge unbalance introduced by the hole separation. A

tendency towards such a phase separation has also been repeatedly observed in other cuprates.

At once, the well developed inhomogeneity and phase separation are inconsistent with the excellent coherence of the lattice demonstrated by the sharpness of many of the Bragg peaks (for example, coherence length over 1000\AA in $\text{La}_{2-x}\text{M}_x\text{CuO}_4$ ¹⁷). However, an appearance of the clearly seen nonphonon X-ray diffuse scattering with unconventional temperature and \mathbf{q} -dependence¹⁷ evidences an occurrence of the local or quasi-local (nanoscale) static and/or dynamic charge inhomogeneity as a possible result of the electronic phase separation. Lack of significant elastic neutron diffuse scattering¹⁷ is compatible with the mainly electronic nature of the inhomogeneity in doped cuprates.

B. Topological phase separation in doped cuprates

The phase separation and electron inhomogeneity are currently considered to be inherent property of lightly doped or so-called under-doped cuprates. Our scenario implies the existence of a critical doping level for the first-order phase transition from parent insulating phase to EHBL phase. EHBL represents the phase state with a condensation of CT excitons. Without any doping such a phase is equivalent to a half-filled hard-core Bose-Hubbard (hc-BH) system. Does new phase is homogeneous or not? We argue that EHBL phase is not only inherently inhomogeneous but this inhomogeneity governs the low-energy physics of doped cuprates. Indeed, the model of the EH Bose-liquid implies that the doped cuprates are proved to be in the universality class of the pseudo-spin 2D systems which description incorporates the inhomogeneity centers like topological defects to be a natural element of essential physics. In addition, it should be noted that the self-trapping of CT excitons with nonzero electric dipole moment is characterized by the nucleation of vortex-like configurations providing the minimum of the dipole-dipole coupling. In other words, the nucleation of the EH Bose liquid implies the formation of different topological textures. However, below we concentrate on the deviation from the half-filling to be seemingly the main driving force of the topological inhomogeneity in doped cuprates.

The hc-BH-model (quantum lattice Bose gas) has a long history and has been suggested initially for conventional superconductors¹⁸, quantum crystals such as ^4He where superfluidity coexists with crystalline order.^{19,20} Afterwards, the Bose-Hubbard model has been studied as a model of the superconductor-insulator transition in materials with local bosons, bipolarons, or preformed Cooper pairs.^{21,22} The most recent interest to the system of hard-core bosons comes from the delightful results on Bose-Einstein (BE) condensed atomic systems.

One of the fundamental hot debated problems in bosonic physics relates the evolution of the charge ordered (CO) ground state of 2D hard-core BH model with

doping away from half-filling. Numerous model studies steadily confirmed the emergence of "supersolid" phases with simultaneous diagonal and off-diagonal long range order while Penrose and Onsager²³ were the first showing as early as 1956 that supersolid phases do not occur.

The most recent quantum Monte-Carlo simulations^{24,25,26} found two significant features of the 2D Bose-Hubbard model with a screened Coulomb repulsion: the absence of supersolid phase at half-filling, and a growing tendency to phase separation (CO-BS) upon doping away from half-filling. Moreover, the checkerboard supersolid phase appears to be unstable thermodynamically.^{24,25,26} Batrouni and Scalettar studied quantum phase transitions in the ground state of the 2D hard-core boson Hubbard Hamiltonian and have shown numerically that, contrary to the generally held belief, the most commonly discussed "checkerboard" supersolid is thermodynamically unstable and phase separates into solid and superfluid phases. The physics of the CO-BS phase separation in Bose-Hubbard model is associated with a rapid increase of the energy of a homogeneous CO state with doping away from half-filling due to a large "pseudo-spin-flip" energy cost. Hence, it appears to be energetically more favorable to "extract" extra bosons (holes) from the CO state and arrange them into finite clusters with a relatively small number of particles. Such a droplet scenario is believed to minimize the long-range Coulomb repulsion.

What is, however, the detailed structure of the CO+BS phase separated state? In the paper²⁷ a topological scenario of CO+BS phase separation has been proposed. The extra bosons/holes doped to a checkerboard CO phase of 2D boson system are believed to be confined in the ring-shaped domain wall of the skyrmion-like topological defect which looks like a bubble domain in antiferromagnet.²⁸ This allows us to propose the mechanism of 2D *topological (CO+BS) phase separation* when the doping of the bare checkerboard CO phase results in the formation of a multi-center topological defect, which simplified pseudo-spin pattern looks like a system of bubble CO domains with Bose superfluid confined in charged ring-shaped domain walls.

Such a skyrmion scenario in hc-BH model allows us to draw several important conclusions. The parent checkerboard CO phase gradually loses its stability under boson/hole doping, while a novel topological self-organized texture is believed to become stable. In other words, away from half-filling one may anticipate the nucleation of topological defect in the unconventional form of the multi-center skyrmion-like object with ring-shaped Bose superfluid regions positioned in antiphase domain wall separating the CO core and CO outside of the single skyrmion. Specific spatial separation of BS and CO order parameters that avoid each other reflects the competition of kinetic and potential energy. Such a *topological (CO+BS) phase separation* is believed to provide a minimization of the total energy as compared with its uniform supersolid counterpart.

The most probable possibility is that every domain wall accumulates single boson, or boson hole. Then, the number of centers in a multi-center skyrmion nucleated with doping has to be equal to the number of doped bosons/holes.

Apparently, the boson/hole doping is likely to be a driving force for a nucleation of a single, or multi-center skyrmion-like self-organized collective mode, which may be (not strictly correctly) referred to as multi-skyrmion system akin in a quantum Hall ferromagnetic state of a two-dimensional electron gas²⁹. We may characterize an individual skyrmion by its position (i.e., the center of skyrmionic texture), its size (i.e., the radius of domain wall), and the orientation of the in-plane components of pseudo-spin (U(1) degree of freedom). An isolated skyrmion is described by the inhomogeneous distribution of the CO parameter, or staggered boson density, charge order parameter characterizing the deviation from the half-filling, and superfluid order parameter with a modulus and phase. As regards the charge distribution, the multi-center topological defects has much in common with a charge-density wave, Wigner crystal or Skyrmion crystal.

It is worth noting that multi-center skyrmions, or multi-skyrmion topological defects in non-linear σ -model were regarded by Belavin and Polyakov.⁷ Interestingly, that such entities may be considered as a system of non-interacting quasiparticles.

It seems likely that any doped particle (boson/holes) results in a nucleation of a new skyrmion, hence its density changes gradually with particle doping. Therefore, as long as the separation between skyrmionic centers is sufficiently large so that the inter-skyrmion interaction is negligible, the energy of the system per particle remains almost constant. This means that the chemical potential of boson or hole remains unchanged with doping and hence apparently remains fixed.

Depending on the doping level we may distinguish three types of topologically phase-separated EHBL in doped cuprates: i) "underdoped" EHBL with weakly coupled skyrmions, when their behavior is ruled mainly by random impurity potential; ii) "optimally doped" EHBL with strongly coupled skyrmions, forming skyrmion liquid, or crystal; iii) "overdoped" EHBL with a complex topological texture that hardly reduces if any to a system of well separated quasiparticles. The illustrative picture of different phase separation regimes in doped cuprates is presented in Fig.1.

III. IR OPTICAL RESPONSE OF THE DOPED CUPRATE. STATIC TOPOLOGICAL PHASE SEPARATION AND EFFECTIVE MEDIUM THEORY

The hole/electron doping into parent cuprate is likely to be a driving force for a growth of primary electron-hole droplets with a stabilization of a single, or multi-center

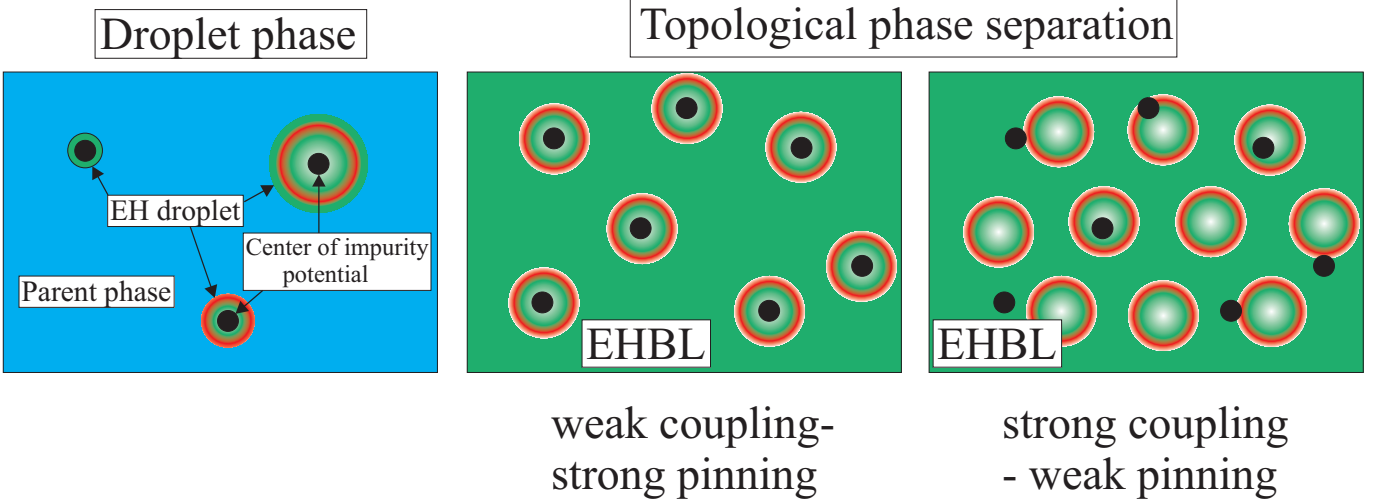


FIG. 1: Illustrative picture of different phase separation regimes in doped cuprates

skyrmion-like EHBL collective mode, followed by a first order phase transition from parent insulating state into unconventional topological EHBL phase. The appropriate evolution of electron structure should manifest itself in optical properties. We believe, that in a broad spectral range the basic features of the optical response of SC oxides can be consistently accounted for proceeding from the unified physical picture of their intrinsic electronic inhomogeneity. Below we focus on optical response in infrared. First we address the response of doped cuprate with a static, or "quenched" phase separation when the crude reasonable model is that of a granular composite, whose constituents have the complex dielectric functions $\varepsilon_i(\omega)$, where i labels the species of the grains. What is to be stressed is that the resulting dielectric function ε_{eff} of the composite does not reduce to the simple weighted average of the form $p\varepsilon_1 + (1-p)\varepsilon_2$, where p is the volume fraction of its first component. The correct averaging can be performed within the effective medium theory and takes into account the specific effects of the resonant scattering and absorption of light at the interfaces of the grains. The corresponding surface plasmon resonances in the optical spectra of the composite media are also referred to as the geometric ones, because their energy is governed by the shape of the inhomogeneities.

Optical measurements in midinfrared (MIR) region provide an important information as regards the low-energy excitations in cuprates. The nature of MIR band in insulating cuprates remains to be one of the old mysteries of the cuprate physics.

At first glance, overall MIR band in insulating cuprates may be assigned to different dipole-allowed CT transitions in EH droplets which certain volume fraction is surely contained in the nominally pure parent cuprates. Generally speaking, the low-frequency optical response of EH droplet is composed from two main contributions, that of intra-band two-center local boson transitions and one-center $^1A_1 \rightarrow ^1E_u$ CT transitions. The former can

form a metallic-like band with the maximal width of the order of 0.1 eV, while the latter represents the complex optical response of single PJT center which typical energy falls in the interval of several tenth of eV. However, the EH droplets are scattered in a highly polarizable surrounding that turns the calculation of their optical response into a very complicated problem. Typical size of the EH droplets seems to fall in the nanoscopic scale. Hence, when considering the phenomena with a relevant characteristic length, e.g. infrared optical absorption ($\lambda = 0.5 - 1.5 \mu\text{m}$), doped cuprates can be roughly regarded as a binary granular medium, composed of two components.

The idea of real-space inhomogeneity is most naturally expressed in terms of an effective medium theory (EMT), which aims to evaluate some property of a composite, those of pure components being given. First, we would like to shortly overview the effective medium theory³⁰ which appears to be a powerful tool for the quantitative description of the optical response of inhomogeneous systems. In its simplest form, the EMT equation for effective dielectric function ε_{eff} of the two-component inhomogeneous system reads as follows³⁰:

$$\int_V dV p(\varepsilon) \sum_{i=1}^3 \frac{\varepsilon - \varepsilon_{eff}}{\varepsilon_{eff} + L_i(\varepsilon - \varepsilon_{eff})} = 0, \quad (1)$$

where the integration runs over the volume of the sample, $p(\varepsilon) = p_1 \delta(\varepsilon(r) - \varepsilon_1) + p_2 \delta(\varepsilon(r) - \varepsilon_2)$. We consider the two components of binary composite on equal footing with $p_{1,2}$ being the volume fractions, $\varepsilon_{1,2}$ and L_i the dielectric functions and the depolarization factors of the grains of its constituents, respectively.

It is worth to emphasize that in effective medium approximation the volume of the droplet does not enter the calculations, but is accounted implicitly in the validity range of the theory, restricting the mean size of the droplet to be smaller than the wavelength. Hence, within

the EMT, the volume fractions $p_{1,2}$ can only change through the number of the droplets rather than due to the variation of their sizes. In general, $p_{1,2}$ are determined by thermodynamical conditions and depend on temperature, pressure, and other external factors. The approach³¹, we employed here to lend more plausibility to this physically transparent EMT scheme, is to take into account the natural difference between the core and the surface properties of the EH droplets using the standard expression for the polarizability of the coated ellipsoid.³²

The spectra of nanoscopically disordered metal-insulator media can display some specific features due to so-called geometric resonances (surface plasmon, or Mie resonances)³⁰, that have no counterpart in homogeneous systems. These arise as a result of resonant behaviour of local field corrections to the polarizability of the granular composite and are governed to a considerable extent by the shape of the grains. The frequency of geometric resonance is then easily obtained as the one at which the polarizability of small particle diverges. For the case of spherical metallic droplets embedded in the insulating matrix with a constant dielectric permittivity ε_d this leads to the equation:

$$\varepsilon(\omega)_m + 2\varepsilon_d = 0, \quad (2)$$

whence the resonance frequency is

$$\omega_r = \frac{\omega_p}{\sqrt{1 + 2\varepsilon_d}}, \quad (3)$$

if simple Drude's expression

$$\varepsilon = \varepsilon_0 - \frac{\omega_p^2}{\omega(\omega + i\gamma)} \quad (4)$$

with the plasma frequency ω_p and the damping parameter γ is assumed for the metallic permittivity. In the case of arbitrary ellipsoid there are three different principal values of polarizability and (3) generalizes to

$$\omega_r^i = \omega_p \sqrt{\frac{L_i}{\varepsilon_d - L_i(\varepsilon_d - 1)}}, \quad i = 1, 2, 3, \quad (5)$$

where L_i are three shape-dependent depolarization factors. The Drude approximation is reasonable and is more general than it may seem, since the form can be regarded as a limiting one of the universal expression for a dynamical conductivity in terms of memory function with ω_p and γ to be effective parameters.

An effective medium theory has been applied for the simulation of the optical spectra of $\text{La}_{2-x}\text{Sr}_x\text{CuO}_4$ with x varying in a wide range³³ (see Fig.2). Imaginary part of dielectric function of parent insulating La_2CuO_4 was fitted to experiment³⁴ by the sum of three Gaussians in a broad spectral range to ensure the validity of its real part, derived via Kramers-Krönig transformation. The phonon bands have been neglected throughout the calculations. The droplets are assumed to have ellipsoidal shape with

the in-plane semi-axes ratio denoted as α and that of out-of-plane and major in-plane semi-axes as β . These geometrical parameters enter the theory through the depolarization factors and were found to affect strongly the dielectric function of doped cuprate.

Left hand side panel in Fig.2 clearly shows the evolution of the low-frequency optical response (MIR-band) given small volume fraction of metallic-like ($\omega_p = 1.9$ eV) disc-shaped droplets with varying effective relaxation rate and volume fraction. For comparison we demonstrate the predictions of a simple additive two-fluid model $\sigma(\omega) = p\sigma_{\text{metal}} + (1-p)\sigma_{\text{insulator}}$ (dotted curves). One may see that the effect of EH droplets dispersed in a polarizable insulating matrix results in a crucial rearrangement of the optical response with the appearance of novel characteristic features such as Mie resonances. It is worth noting that in terms of EMT approach the appearance of metallic-like EH droplets in insulating matrix leads to the crucial red-shift of the effective insulating gap of doped cuprate. In a sense, for lightly doped cuprates one might say about two characteristic insulating gaps.

The model in its simplest form³³ was found able to reproduce all essential features of the transmittance³⁵, optical conductivity $\sigma(\omega)$, and EELS spectra³⁴ for 214 system. It is easily concluded after simple comparison of the data presented in central and right hand side panels of Fig.2. Substantial difference in the spectral and doping dependence of optical conductivity for thin-film³⁵ and bulk samples³⁴ is easily explained assuming different shape of metallic and dielectric regions in both materials. New peaks in $\sigma(\omega)$ and absorption spectra, that emerge in the mid-infrared range upon doping are attributed to surface plasmon resonances and its interference with different charge transfer transitions in EH droplets.

Overall, one may conclude that the MIR optical response of insulating cuprates strongly supports the EH droplet scenario with an intrinsic metallic-like transport.

IV. IR OPTICAL RESPONSE OF THE DOPED CUPRATE. DYNAMICS OF TOPOLOGICAL DEFECT IN A RANDOM POTENTIAL

The topological structure of EHBL must be considered as being largely dynamic in nature. Underdoped EHBL can be considered to form a system of weakly coupled quasiparticles (skyrmions) exposed to the action of a random potential. We believe, that the model of 2D Bose gas in a random potential offers the most close physical analogy to our case, and we adopt it as the effective model to describe the effects of dynamics of topological defect in the cuprates.

Below we'll address the approximation of slow topological dynamics with characteristic energies much lower than the effective insulating gap of doped cuprate.

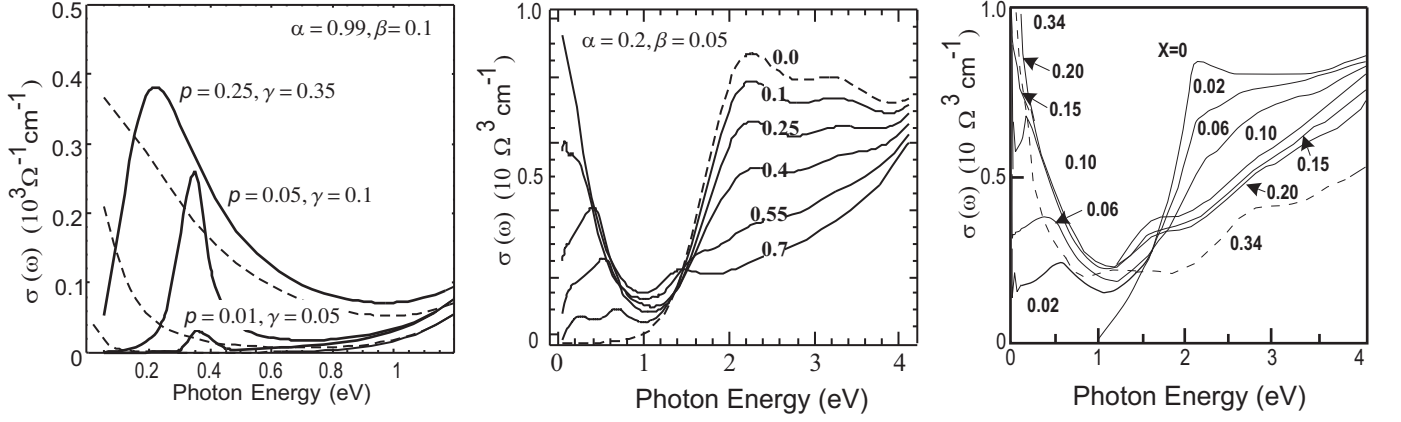


FIG. 2: Optical conductivity of doped 214 cuprate in frames of the effective medium theory. Left hand side panel shows the evolution of the low-frequency optical response given small volume fraction of metallic-like droplets and varying effective relaxation rate. Central panel: calculated optical conductivity for different volume fractions of metallic phase. The numbers against the curves stand for the relative volume fraction p of the quasi-metal phase. Right hand side panel: measured optical conductivity of $\text{La}_{2-x}\text{Sr}_x\text{CuO}_4$ for different x [34]. The numbers against the curves stand for the doping level.

A. The memory function technique.

An adequate formalism for the description of the overdamped charge dynamics in presence of a strong disorder was elaborated by W. Götze and coworkers^{36,37}, who showed, that the optical conductivity $\sigma(\omega)$ at both sides of Anderson transition can be expressed in a general form:

$$\sigma' + i\sigma'' = i \frac{\omega_p^2}{\omega + M(\omega)} \quad (6)$$

where ω_p is the plasma frequency, $M(\omega) = M' + iM''$ is the memory function. With $M = i\gamma = \text{const}$ this expression reduces to the simple Drude formula (??). Thus, the Drude model can be understood as a crudest approximation, when the processes of the current dissipation act equally in the whole spectral range and do not depend on the frequency.

The real part of the conductivity σ' , henceforth denoted as σ , may be parameterized in terms of the so called generalized Drude formula³⁶,

$$\sigma(\omega) = \frac{\Omega_p(\omega)^2 \Gamma(\omega)}{\omega^2 + \Gamma(\omega)^2}, \quad (7)$$

where the renormalized plasma frequency $\Omega_p(\omega)$ and the relaxation rate $\Gamma(\omega)$ have the form:

$$\Omega_p(\omega) = \omega_p / \sqrt{\eta(\omega)}, \quad \gamma(\omega) = M''(\omega) / \eta(\omega), \quad (8)$$

$$\eta(\omega) = 1 + M'(\omega) / \omega. \quad (9)$$

The cornerstone result of the approach is based on the mode coupling self-consistency relation of the memory function and the impurity potential in the momentum space³⁷:

$$M(\omega) = \frac{1}{nm} \int \frac{\Phi_0(k, \omega + M(\omega))}{1 + M(\omega) \Phi_0(k, \omega + M(\omega)) / \chi(k=0, \omega)} k^2 \langle |U(q)|^2 \rangle d\mathbf{k}, \quad (10)$$

where n , m are the concentration and the mass of the carriers, Φ_0 is the density-density correlation function in absence of the impurities, expressed through the generalized susceptibility $\kappa(q, z)$:

$$\Phi_0(q, z) = \frac{1}{z} (\kappa(q, z) - \kappa(q)_{z=0}). \quad (11)$$

Within the linear response theory $\kappa(q, z)$ is obtained from

the familiar expression:

$$\kappa = - \lim_{\alpha \rightarrow 0} \sum_q \frac{f(\varepsilon_{k+q}) - f(\varepsilon_q)}{\varepsilon_{k+q} - \varepsilon_q - \omega - i\alpha}, \quad (12)$$

where ε_k is the energy of the particles and f is their partition function. Other quantities in Eq. (10) are the concentration n and the mass m of the charge carriers.

Now, dwell upon the quantity $\langle |U(q)|^2 \rangle$. This is the average squared Fourier transform of the random poten-

tial $U(\mathbf{r})$, defined a superposition of the partial impurity potential u , each centered at the sites \mathbf{r}_i :

$$U(\mathbf{r}) = \sum_i u(\mathbf{r} - \mathbf{r}_i), \quad (13)$$

where the sum is over the impurity sites. Hence,

$$\langle |U(q)|^2 \rangle = |u(q)|^2 s(q) \quad (14)$$

$$s(q) = \left\langle \sum_{i,j} e^{i\mathbf{q}(\mathbf{r}_i - \mathbf{r}_j)} \right\rangle, \quad (15)$$

where the brackets denote the averaging over the impurity sites. In what follows, we shall consider the case of random impurities. Then, the structure factor $s(q)$ becomes trivial and reduces to n_i , the concentration of impurities, whence

$$\langle |U(q)|^2 \rangle = n_i |u(q)|^2. \quad (16)$$

In zero temperature limit, the machinery of the correlation functions of free 2D Bose gas is easily implemented because of the particularly simple analytic form of the generalized susceptibility³⁸:

$$\kappa_0(k, z) = \frac{2n\varepsilon_k}{\varepsilon_k^2 - z^2}, \quad (17)$$

where $\varepsilon_k = k^2/2m$ is the dispersion of free particles.

To proceed further, it is convenient to introduce the dimensionless variables, labeled with tilda ($\widetilde{\cdot}$) to distinguish them from their dimensional counterparts. We have chosen for the units of the mass and the charge the corresponding quantities for the free electron (m_e , e). Aiming to simplify the calculations, we adopt the unit of the wave vector as $q^* = (8\pi n/a^*)^{1/3}$, where $a^* = \hbar^2 \varepsilon / m e^2$ is the effective Bohr radius³⁹, ε is the static dielectric constant of the medium. The unit of energy is then naturally defined as $E^* = \hbar^2 q^{*2} / 2m_e$. Furthermore, the complex optical conductivity takes the form:

$$\sigma' + i\sigma'' = \sigma^* \frac{i}{\widetilde{\omega} + \widetilde{M}(\widetilde{\omega})}, \quad (18)$$

$$\sigma^* = \frac{\omega_p^2}{E^*} = \frac{1}{E^*} \frac{n_{3D} e^2}{m}, \quad (19)$$

where $\widetilde{\omega} = \omega/E^*$, $\widetilde{M} = M/E^*$, n_{3D} being the volume fraction of the droplets. Under moderate doping, we believe this quantity to be directly related to the doping level x :

$$n_{3D} = \frac{x}{\Delta^2 d}, \quad (20)$$

where Δ is the lattice constant of the CuO_2 plane, d is the interplane spacing.

Taking into account the numerical values of m_e , e_e and \hbar , the final expressions for the adopted units read as

follows:

$$q^* = 3.62 \cdot 10^8 \times \left(\frac{\widetilde{m} \widetilde{e}^2 x}{\varepsilon \Delta^2} \right)^{1/3} \text{ cm}^{-1}, \quad (21)$$

$$E^* = 49.87 \times \left(\frac{\widetilde{e}^2 x}{\varepsilon \Delta^2 \sqrt{\widetilde{m}}} \right)^{2/3} \text{ eV}, \quad (22)$$

$$\sigma^* = 4.0 \cdot 10^3 \times \left(\frac{\widetilde{e}^2 \varepsilon^2 x}{\Delta^2 d^3 \widetilde{m}^2} \right)^{1/3} \Omega^{-1} \text{ cm}^{-1}, \quad (23)$$

where we made use of the relation $1 \text{ eV} \simeq 1.824 \cdot 10^3 \Omega^{-1} \text{ cm}^{-1}$. Let us estimate their possible numerical values. Consider the situation, when the EHBL phase is composed of the heavy Bose particles carrying double elementary charge, $\widetilde{m} = 10$, $\widetilde{e} = 2$. Given the parameters of $\text{La}_{2-x}\text{Sr}_x\text{CuO}_4$ unit cell, $\Delta \simeq 4 \text{ \AA}$, $d \simeq 6 \text{ \AA}$, and the bare dielectric constant $\varepsilon = 40$, we obtain for slight doping $x = 0.01$ the following units of energy and conductivity: $E^* \simeq 294.5 \text{ cm}^{-1}$, $\sigma^* \simeq 0.23 \cdot 10^3 \Omega^{-1} \text{ cm}^{-1}$.

Making use of these notations, it is straightforward to write down the explicit expressions of the correlation functions of the theory:

$$\kappa(q, z) = (2n/E^*) \widetilde{\kappa}(\widetilde{q}, \widetilde{z}) \quad (24)$$

$$\Phi(q, z) = (2n/E^{*2}) \widetilde{\Phi}(\widetilde{q}, \widetilde{z}) \quad (25)$$

$$(z = E^* \widetilde{z}, q = q^* \widetilde{q}),$$

where the frequency and wave vector dependencies are contained in dimensionless expressions:

$$\widetilde{\kappa}(\widetilde{q}, \widetilde{z})_{RPA} = \frac{\widetilde{q}^2}{\widetilde{q}^4 + \widetilde{q} - \widetilde{\omega}^2}, \quad (26)$$

$$\widetilde{\Phi}(\widetilde{q}, \widetilde{z} + \widetilde{M}) = \frac{\widetilde{q}(\widetilde{z} + \widetilde{M})}{(1 + \widetilde{q}^3)(\widetilde{q} + \widetilde{q}^4 - (\widetilde{z} + \widetilde{M})\widetilde{z})}, \quad (27)$$

and

$$\kappa(k, z)_{RPA} = \frac{\kappa(k, z)}{1 + 2\pi e^2 \kappa(k, z)/k} \quad (28)$$

takes into account the 2D Coulomb interaction of quasi-particles in a random phase approximation.

It is also convenient to isolate the dimensionless \widetilde{q} -dependence in the impurity potential:

$$u(q) = U_0 f(\widetilde{q}), \quad (29)$$

where U_0 has the dimension of energy and f specifies the shape of the potential. Finally, the dimensionless analogue of Eq. (10) has the form:

$$\widetilde{M} = \Upsilon \int_0^\infty d\widetilde{q} \widetilde{q}^3 \widetilde{\Phi}(\widetilde{q}, \widetilde{z} + \widetilde{M}) |f(\widetilde{q})|^2, \quad (30)$$

Thus, the dimensionless memory function is governed by the only parameter, which is defined as: $\Upsilon = 4\widetilde{U}_0^2 n_i/n$, where \widetilde{U}_0 , measured in units of E^* , is the strength of the potential (the depth of the potential well), n_i and n are the concentration of the impurities and the carriers, respectively.

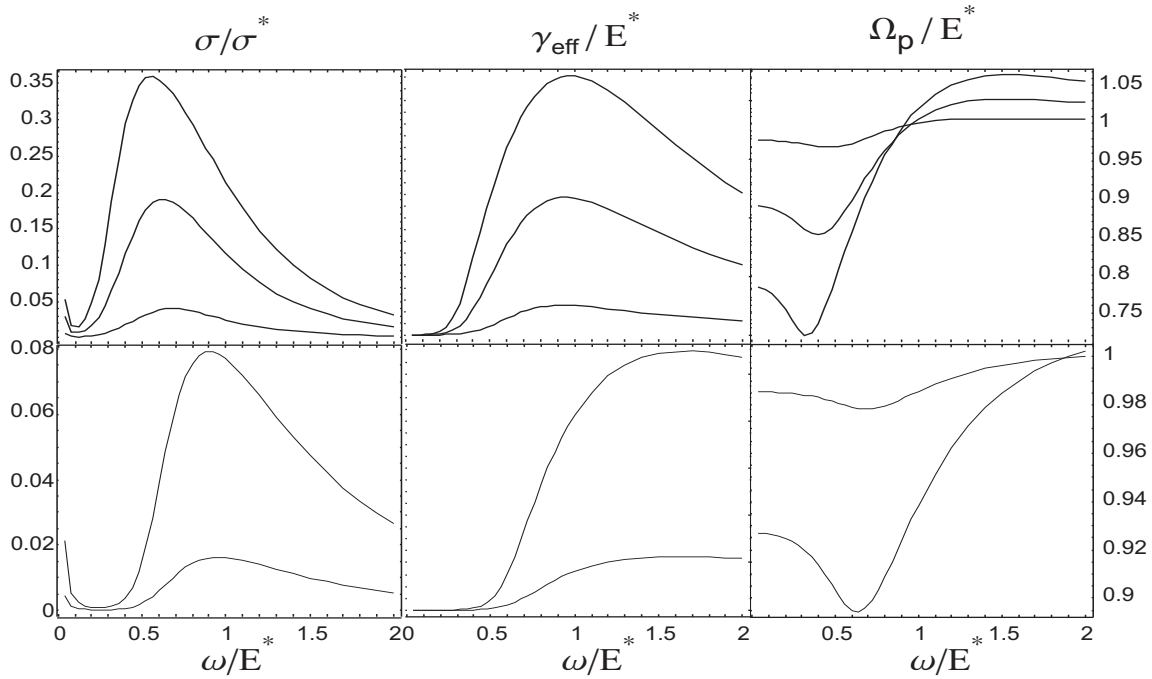


FIG. 3: Dimensionless optical conductivity and the parameters of the generalized Drude expression (8) for different strength of disorder (upper curves correspond to stronger disorder). Upper row: Coulomb impurities. Lower row: Debye impurities.

B. Model simulations

1. Point charges in random potential.

The Eqs. (27 - 30) provide the practical scheme to calculate the optical response of the system in presence of the random potential. We begin by considering the case of the usual 2D charged Bose gas in random potential.

Two especially interesting cases of the impurity potentials have been examined. The first one is the case of Coulomb impurities, located at a certain distance h over the CuO_2 planes: $u(r) = U_0 (R^2 + h^2)^{-1/2}$, where R is the in-plane projection of r . The 2D Fourier transform of the potential is $u(q) = U_0 \exp(-qh)/q$. The second case we considered here corresponds to the Debye impurities, $u(r) = U_0 \exp(-r/r_0)/r$, where r_0 is the screening length. The Fourier transform is $u(q) = U_0 r_0 (1 + q^2 r_0^2)^{-1/2}$.

The overall view of dimensionless spectral dependencies of optical conductivity, effective relaxation rate $\Gamma(\omega)$ and the effective plasma frequency $\Omega_p(\omega)$ (7, 8) is shown in Fig. 3. It can be seen, that the conductivity spectrum is characterized by a broad asymmetric feature due to plasma oscillations of quasiparticles in the potential wells at the plasma frequency, and is not very sensitive to the choice of the profile of the wells, specified by the impurity potential. The stronger is the localization, the sharper is the plasma peak. Because of the total spectral weight conservation, $\int_0^\infty \sigma(\omega) d\omega = \text{const}$, this implies the transfer of the intensity from the coherent response of the condensate $\propto \delta(\omega)$ to the plasma modes.

To be noted is a strong frequency dependence of effective relaxation rate $\Gamma(\omega)$ with nearly constant slope in a wide range, reminiscent of the marginal Fermi liquid behaviour of the cuprates.

The comparison with the previously studied 3D Bose gas³⁹, 3D and 2D Fermi gas^{37,40} makes it possible to conclude, that the response of localized carriers always remains essentially the same. Still more nontrivial is, however, the resemblance of these spectra with those, obtained for pinned charge density waves⁴¹ and Wigner crystals⁴². It seems, that there is a certain dualism between the collective modes of localized charges and pinned phase degrees of freedom.

2. Skyrmion-like quasiparticles in a random potential.

As far as we treat the real-space electronic inhomogeneity in oxides within the effective model of 2D Bose gas, the basic results of previous section hold also for this case.

However, the topological texture of EHBL phase is not the system of structureless point quasiparticles, but rather skyrmion-like entities with a complicated internal structure. Hence, the explicit form of the effective random potential does not remain as simple as what follows from the Coulomb law. Nevertheless, among the possible interactions of the charged impurity with the inhomogeneity the direct electrostatic one is of prime importance.

It is possible to model the charge distribution within

the quasiparticle in a direct manner, assigning the charge density ρ_i to its point (Fig. ??), if the discrete nature of the quasiparticle in the CuO_2 is taken into account. The interaction of an impurity with the quasiparticle is obtained, summing over "internal" coordinates of the quasiparticle (see Eq. (29)):

$$u(\mathbf{r}) = \sum_i \rho_i U_0 f(\mathbf{r} - \mathbf{r}_i), \quad (31)$$

whence the Fourier transform is straightforwardly obtained:

$$u(\mathbf{k}) = U_0 f(k) F(\mathbf{k}), \quad (32)$$

where

$$F(\mathbf{k}) = \sum_l \rho_l \exp(i \mathbf{k} \cdot \mathbf{r}_l) \quad (33)$$

is the form-factor of the droplet and $f(k) = e^{-k h}/k$ for Coulomb impurities, randomly spread at a distance h over the CuO_2 planes.

For the applications, we have to calculate the expression $\langle |F(k)|^2 \rangle$, averaged over the orientations of the quasiparticles. To this end, the additional physical assumptions about the arrangement of the quasiparticle within the CuO_2 plane is required. Since there are *a priori* no reasons to expect some ordering of the quasiparticle, we consider below the case of they random orientations. In two dimensions, we obtain:

$$\langle |F(k)|^2 \rangle = \frac{1}{2\pi} \int_0^{2\pi} \sum_{ij} \rho_i \rho_j e^{i k (r_i - r_j) \cos \varphi} d\varphi = \sum_{ij} \rho_i \rho_j J_0(k r_{ij}), \quad (34)$$

where $r_{ij} = |\mathbf{r}_i - \mathbf{r}_j|$ is the distance between two arbitrary internal points of the quasiparticle, J_0 is the Bessel function of the first kind.

The form-factor of the quasiparticle enables us to investigate a number of the charge configurations of particular interest, such as the charged linear stripes etc., of course with reserve, that only the details of radial charge distribution enter the average form-factor.

It is therefore instructive to consider first the simple case, when the charge distribution in a quasiparticle has the form of an uniform ring with inner radius R_1 and outer radius R_2 . We denote their ratio as $\alpha = R_1/R_2$. Changing α continuously from 0 to 1, we can model both the disk, the thin hook and the intermediate ring configurations. The continuous counterpart of Eq. (34) reads:

$$\langle |F(k)|^2 \rangle(q) = \left(2\pi \int_{R_1}^{R_2} r \rho(r) J_0(q r) dr \right)^2, \quad (35)$$

where $\rho = Q/\pi(R_2^2 - R_1^2)$ – is the (constant) charge density, Q is the full charge of the ring.

A series of model optical conductivity spectra, calculated for the ring geometry of charge distribution in skyrmion-like quasiparticle, is depicted at Fig. 4. It shows the spectra of the bosonic quasiparticles (mass $m = 2m_e$, charge $2e$) distributed within the CuO_2 plane

with the concentration $n_{2D} = 3.5 \cdot 10^{-3} \text{ \AA}^{-2}$ and trapped by the potential induced by Coulomb impurities randomly located at the height $\sim 3 \text{ \AA}$ above CuO_2 plane with the mean wells depth $\sim 1500 \text{ cm}^{-1}$. The value of the static dielectric constant $\varepsilon = 40$ was used in the calculation. The outer radius of rings was fixed to be 30 \AA .

As the aperture of the ring increases, its outer radius kept constant, the intensity of the plasma peak progressively drops because the charge gradually moves away from the impurity. In other words, the larger is the quasiparticle, the weaker it is trapped by the potential. However, the increase of the quasiparticle extent does not simply reduce to its gradual delocalization. It can be seen, that spectrum of the plasma peak of the ring decays into the oscillating structure, that becomes more pronounced as the ring gets thinner. This means, that the inhomogeneous charge distribution in the quasiparticle leads to the complicated profile of the collective mode spectrum with a fine resonant structure. To get insight into the nature of these oscillations, we remember, that the frequency dependence of the memory function $M(\omega)$ is obtained, according to Eq. (30), as a result of the integration of a complicated density fluctuation correlation functions over the momentum space. Taking account of the form-factor of quasiparticle can be interpreted as the evaluation of the memory function using the same integrand, as for the case of structureless point particles, now with a highly nontrivial k -dependent plasmon density of states, that is tantamount to the modification of the dispersion relation of the quasiparticles as distinct from the

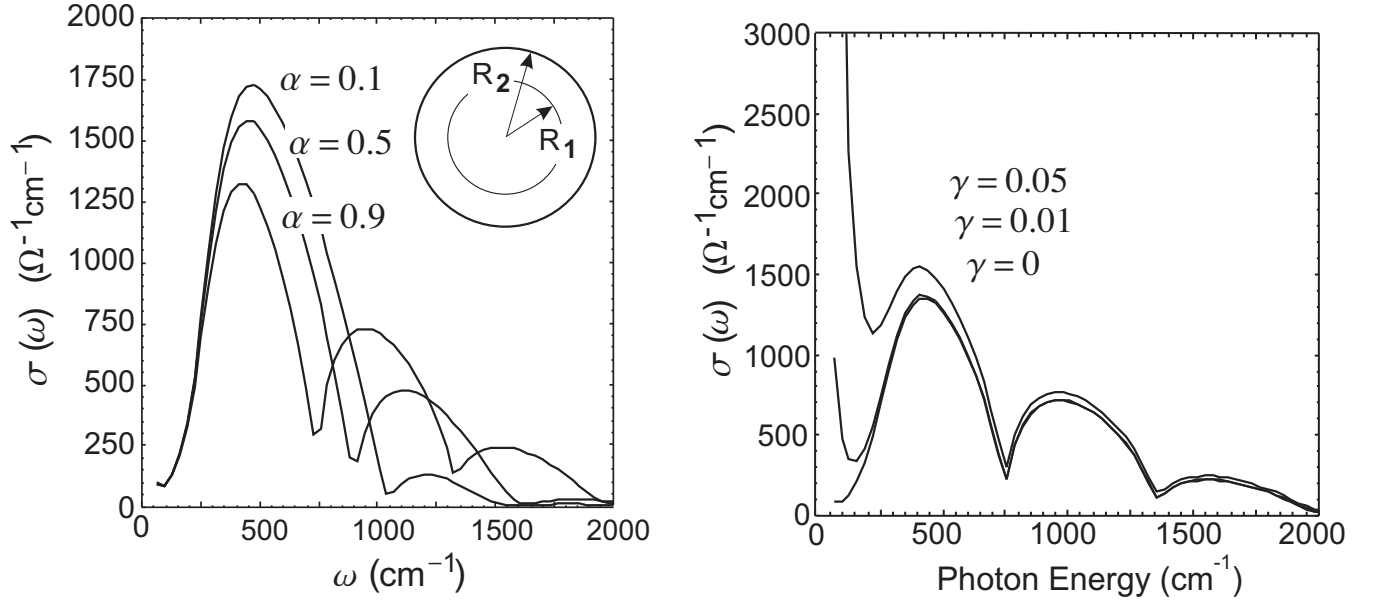


FIG. 4: The optical conductivity of the skyrmion-like quasiparticles with the ring-shaped charge distribution in a random potential. Left panel illustrates the role of different inner-to-outer radius ratio denoted by α . Right panel illustrates the role of different values of the bare relaxation parameter $\gamma_0 = 0.0, 0.01$, and 0.05 eV given $\alpha = 0.9$

case of the free Bose gas.

The result obtained is to be compared with the microwave optical conductivity of lightly doped $\text{La}_{2-x}\text{Sr}_x\text{CuO}_4$ ⁴³ ($x = 0.015$). The multi-peak structure of calculated spectra falls in nearly the same spectral range, as that, observed in experiment. The authors of the paper [43] regard the resonances in optical conductivity to be the manifestation of the pinned Wigner crystal response of the carriers in CuO_2 planes. We believe, that our results could provide another (quantitative) interpretation of these experimental findings in terms of the plasma oscillations of the quasiparticles phase, trapped in the roughness of a complicated non-uniform potential landscape.

The memory function approach considered here enables us to model the optical response of the quasiparticles due to their collective plasma modes. Of course, there are also another channels of the dissipation in a phase-separated systems, related to the excitations of other degrees of freedom, that are beyond the scope of the present analysis. We may try to get idea of the role of this additional absorption mechanisms phenomenologically, inserting an additional relaxation term in the denominator of the generalized Drude formula. This trick reflects the fact, that different mechanisms of current relaxation act nearly independently. Having in mind to minimize the number of model assumptions, we consider the following trial formula

$$\sigma(\omega) = \text{Re} \frac{\Omega_p^2}{\omega + M(\omega) + i\gamma_0}, \quad (36)$$

where $\gamma_0 = \text{const}$. Note that the trivial memory function $M = i\gamma_0$ corresponds to the conventional Drude formula.

The right hand side panel in Fig. 4 illustrates the effect of a gradual increase of the bare relaxation parameter γ_0 on the optical conductivity of the "ring-shaped" quasiparticles. In absence of γ_0 the optical conductivity displays the broad plasma feature and pseudogap depression of the spectrum at lower frequencies. Turning on γ_0 leads to the development of the Drude like tail within the gap.

It is interesting to note that such a spectral behavior is actually observed for different cuprates (see e.g. Ref.44) with varying the temperature. It may be seen, that the inclusion of additional dissipation channel allows to simulate the temperature effect.

V. CONCLUSION

We consider the cuprates to be unconventional systems which are unstable with regard to a self-trapping of the low-energy charge transfer excitons with a nucleation of EH droplets being actually the system of coupled electron CuO_4^{7-} and hole CuO_4^{5-} centers having been glued in lattice due to strong electron-lattice polarization effects. The hole/electron doping into parent cuprate is likely to be a driving force for a growth of primary EH droplets with a gradual stabilization of a single, or multi-center skyrmion-like EH Bose liquid collective mode, followed by a first order phase transition from parent insulating state into unconventional topological EH Bose liquid phase. The latter is believed to be described as a system of interacting skyrmion-like entities which concentration is specified by the doping. Nanoscopic electron inhomogeneity is believed to be inherent property

of doped cuprates throughout the phase diagram beginning from EH droplets in insulating parent system and ending by a topological phase separation in EHBL phase.

We have examined the effects of electron inhomogeneity accompanying such a phase separation on IR optical conductivity. A simple model of metal-insulator composite and effective medium theory has been used to describe the static phase separation effects. Specific effects of spectral weight red-shift with the appearance of low-energy effective insulating gap, the seeming "quenching" of effective plasmon frequency, and the emergence of MIR bands have been assigned to the effects of phase separation.

The low-frequency dynamics of topological EHBL phase in a random potential in underdoped regime has been discussed in a quasiparticle approximation in frames of the memory function formalism. The appropriate low-

frequency optical conductivity appears to have anomalous many-peak "non-Drude" spectral dependence that resembles that of observed experimentally.

The effects of static and dynamic nanoscopic phase separation are believed to describe the main peculiarities of the optical response of doped cuprates in a wide spectral range.

Acknowledgments

Authors acknowledge the support by SMWK Grant, INTAS Grant No. 01-0654, CRDF Grant No. REC-005, RME Grant No. E02-3.4-392 and No. UR.01.01.042, RFBR Grant No. 01-02-96404.

-
- * Electronic address: eugene.zenkov@usu.ru
- ¹ S.H. Pan, J.P. O'Neal, R.L. Badzey *et al.*, *Nature*, **413**, 282 (2001)
 - ² K. M. Lang, V. Madhavan, J. E. Hoffman *et al.*, *Nature*, **415**, 412 (2002)
 - ³ *Relaxations of Excited States and Photo-Induced Structural Phase Transitions*, ed.: K. Nasu, Springer Series in Solid-State Sciences, V. 124, p.17 (1997).
 - ⁴ A.L. Shluger and A.M. Stoneham, *J. Phys.: Condens. Matter* **5** 3049 (1993).
 - ⁵ V.S. Vikhnin, S. Avanesyan, H. Liu, S.E. Kapphan, J. Phys. Chem. Solids, **63**, 1677 (2002).
 - ⁶ F.C. Zhang, K.K. Ng, *Phys. Rev. B* **58**, 13520 (1998).
 - ⁷ A.S. Moskvina, R. Neudert, M. Knupfer, J. Fink, and R. Hayn, *Phys. Rev. B* **65**, 180512(R) (2002).
 - ⁸ A.S. Moskvina, M. Knupfer, R. Neudert *et al.* (unpublished)
 - ⁹ T.M. Rice, in *Solid State Physics*, Eds. H. Ehrenreich, F. Seitz, D. Turnbull, **32**, 1 (1977).
 - ¹⁰ A.S. Moskvina, *JETP Lett.*, **58**, 342 (1993).
 - ¹¹ A.S. Moskvina, *Physica B*, **252**, 186 (1998).
 - ¹² V. J. Emery, S. A. Kivelson, and O. Zachar, *Phys. Rev. B* **56**, 6120 (1997).
 - ¹³ V. J. Emery, S.A. Kivelson, *Physica C*, **209**, 597 (1993); *Nature*, **374**, 434 (1995); *Phys. Rev. Lett.* **74**, 3253 (1995).
 - ¹⁴ E.W. Carlson, V. J. Emery, S. A. Kivelson, and D. Orgad, *arXiv:cond-mat/0206217*.
 - ¹⁵ T. Egami, *J. Low Temp. Phys.* **105**, 791 (1996).
 - ¹⁶ J. M. Tranquada *et al.*, *Phys. Rev. B* **50**, 6340 (1994).
 - ¹⁷ E. D. Isaacs, G. Aeppli, P. Zschack *et al.*, *Phys. Rev. Lett.*, **72**, 3421 (1994); W. Dmowski, R.J. McQueeny, T. Egami *et al.*, *Phys. Rev.*, **B52**, 6829 (1995).
 - ¹⁸ M.R. Schafroth, *Phys. Rev.* **100**, 463 (1955).
 - ¹⁹ H. Matsuda and T. Tsuneto, *Suppl. Prog. Theor. Phys.* **46**, 411 (1970).
 - ²⁰ K. Liu and M. Fisher, *J. Low Temp. Phys.* **10**, 655 (1973).
 - ²¹ Kenn Kubo and Satoshi Takada, *J. Phys. Soc. Jap.*, **52**, 2108 (1983).
 - ²² R. Micnas, J. Ranninger and S. Robaszkiewicz, *Rev. Mod. Phys.* **62**, 113 (1990).
 - ²³ O. Penrose and L. Onsager, *Phys. Rev.* **104**, 576 (1956).
 - ²⁴ G. G. Batrouni and R. T. Scalettar, *Phys. Rev. Lett.* **84**, 1599 (2000).
 - ²⁵ F. Hébert, G.G. Batrouni, R.T. Scalettar *et al.*, *Phys. Rev. B* **65**, 014513 (2001).
 - ²⁶ Guido Schmid, Synge Todo, Matthias Troyer, and Ansgar Dorneich, *Phys. Rev. Lett.* **88**, 167208-1 (2002).
 - ²⁷ A.S. Moskvina, I.G. Bostrem, A.S. Ovchinnikov, unpublished
 - ²⁸ A.S. Ovchinnikov, I.G. Bostrem, A.S. Moskvina, *Phys. Rev. B* **66**, 134304 (2002).
 - ²⁹ A. G. Green, *arXiv:cond-mat/0002053*; *Phys. Rev. B* **61**, R16299 (2000).
 - ³⁰ David J. Bergman and David Stroud, in *Solid State Physics*, H. Ehrenreich and D. Turnbull, Eds., **46**, 148 (1992).
 - ³¹ Ping Sheng, *Phys. Rev. Lett.* **45**, 60 (1980)
 - ³² R.R. Bilboul, *Brit. J. Appl. Phys. (J. Phys. D)*, **2**, 921 (1969)
 - ³³ A. S. Moskvina, E. V. Zenkov and Yu. D. Panov, *J. Luminescence*, **94-95**, 163 (2001)
 - ³⁴ S. Uchida, T. Ido, H. Takagi *et al.*, *Phys. Rev. B* **43**, 7942 (1991).
 - ³⁵ M. Suzuki, *Phys. Rev. B* **39**, 2321 (1989).
 - ³⁶ W. Götze, P. Wölfe, *Phys. Rev. B* **6**, 1226 (1972)
 - ³⁷ W. Götze, *Phil. Mag. B*, **43**, 219, (1981)
 - ³⁸ D.F. Hines, N.E. Frankel, *Phys. Rev. B* **20**, 972 (1979)
 - ³⁹ A. Gold, *Phys. Rev. A* **33**, 652 (1986)
 - ⁴⁰ A. Gold, W. Götze, *Phys. Rev. B* **33**, 2495 (1986)
 - ⁴¹ H. Fukuyama, P.A. Lee, *Phys. Rev. B* **17**, 535 (1978)
 - ⁴² R. Chitra, T. Giamarchi, and P. Le Doussal, *Phys. Rev. Lett.* **80**, 3827, (1998)
 - ⁴³ Y.H. Kim, P.H. Hor, *Mod. Phys. Lett.*, **15**, 497 (2001)
 - ⁴⁴ T. Startseva, T. Timusk, M. Okuya, T. Kimura, K. Kishio, *Physica C*, **321**, 135, (1999)